Biogeosciences Discuss., 11, 15053–15086, 2014
www.biogeosciences-discuss.net/11/15053/2014/
doi:10.5194/bgd-11-15053-2014

Biogeosciences Discussions
Open Access

Microbial iron uptake in the naturally fertilized waters in the vicinity of Kerguelen Islands: phytoplankton–bacteria interactions

M. Fourquez[1,2,3], **I. Obernosterer**[2,3], **D. M. Davies**[4,5], **T. W. Trull**[4,5], **and S. Blain**[2,3]

[1]Institute for Marine and Antarctic Studies, University of Tasmania, Hobart 7001, Australia
[2]Sorbonne Universités, UPMC Univ Paris 06, UMR 7621, Laboratoire d'Océanographie Microbienne (LOMIC), Observatoire Océanologique, 66650 Banyuls/mer, France
[3]CNRS, UMR 7621, Laboratoire d'Océanographie Microbienne, Observatoire Océanologique, 66650 Banyuls/mer, France
[4]CSIRO Oceans and Climate Flagship, Hobart 7001, Australia
[5]Antarctic Climate and Ecosystems Cooperative Research Centre, Hobart 7001, Australia

Received: 7 October 2014 – Accepted: 7 October 2014 – Published: 24 October 2014

Correspondence to: M. Fourquez (marion.fourquez@utas.edu.au)

Published by Copernicus Publications on behalf of the European Geosciences Union.

Abstract

Iron (Fe) uptake by the microbial community and the contribution of three different size-fractions was determined during spring phytoplankton blooms in the naturally Fe fertilized area off Kerguelen Islands (KEOPS2). Total Fe uptake in surface waters was on average 34 ± 6 pmol Fe L^{-1} d^{-1}, and microplankton (> 25 µm size-fraction; 40–69 %) and pico-nanoplankton (0.8–25 µm size-fraction; 29–59 %) were the main contributors. The share of heterotrophic bacteria (0.2–0.8 µm size-fraction) to total Fe uptake was low at all stations (1–2 %). Iron uptake rates normalized to carbon biomass were highest for pico-nanoplankton above the Kerguelen plateau and for microplankton in the downstream plume. We also investigated the potential competition between heterotrophic bacteria and phytoplankton for the access to Fe. Bacterial Fe uptake rates normalized to carbon biomass were highest when bacteria were incubated in the absence of both micro- and pico-nanoplankton. The absence of microplankton resulted in a decrease in bacterial Fe uptake rates by up to 20-fold, while in incubations with the whole microbial community bacterial uptake rates were reduced by 2- to 8-fold. In Fe-fertilized waters, the bacterial Fe uptake rates normalized to carbon biomass were positively correlated with primary production. Taken together, these results demonstrate that heterotrophic bacteria are outcompeted by small sized phytoplankton cells for the access to Fe during the spring bloom development, most likely due to the limitation by organic matter. We conclude that the Fe and carbon cycles are tightly coupled and driven by a complex interplay of competition and synergy between different members of the microbial community.

1 Introduction

Microorganisms in the ocean are characterized by widespread distributions, large abundances and high metabolic rate activities. Consequently they play a pivotal role in biogeochemical cycles of many elements (Arrigo, 2005; Madsen, 2011). Following

BGD
11, 15053–15086, 2014

the pioneering work of Martin et al. (1998), a major achievement in the past decades has been the discovery of the tight, but complex link between the carbon and iron (Fe) biogeochemical cycles in the ocean. Thus, it is not surprising that microorganisms play a crucial role in the functioning and the coupling of both cycles. Autotrophs are a net carbon dioxide (CO_2) sink and heterotrophs are a net CO_2 source, but both require Fe to process carbon. Therefore, the balance between autotrophy and heterotrophy and ultimately the air–sea CO_2 flux should be influenced by Fe availability for microorganisms. This issue is definitively critical in environments receiving low Fe supply, like the high nutrient low chlorophyll regions (HNLC).

The role of heterotrophic bacteria has been far less studied than that of phytoplankton. However, essential data for the understanding of the responses of heterotrophic bacteria to Fe limitation have already been collected. Iron uptake rates, Fe cellular contents and Fe / carbon ratios were determined in various environments (Tortell et al., 1996; Maldonado et al., 2001; Sarthou et al., 2008). Culture experiments (Granger and Price, 1999; Fourquez et al., 2014) have elucidated some of the metabolic pathways affected by Fe limitation which may explain the changes observed in Fe-limited heterotrophic cells or communities. Additionally, the obligate requirement of Fe for heterotrophic bacteria and phytoplankton suggests that both organisms are competing for Fe acquisition. The competition between phytoplankton and bacteria was addressed experimentally (Mills et al., 2008) and conceptually (Litchman et al., 2004) for the access to nitrogen and phosphorus, but this issue has been rarely studied in the case of Fe (Boyd et al., 2012). Beside this possible pure competition, both autotrophic and heterotrophic microorganisms, could also benefit from each other. Phytoplankton are a source of carbon for heterotrophic bacteria and the production of ligands by these latter could make Fe available for other microorganisms (Amin et al., 2009; Hassler et al., 2011a, b). The aim of our study was to investigate further the complex interactions between heterotrophic bacteria and phytoplankton, with respect to the carbon and Fe cycling.

BGD
11, 15053–15086, 2014

The Southern Ocean is the largest HNLC region in the world ocean. However, at several places, natural Fe fertilization sustains massive blooms (Blain et al., 2007; Pollard et al., 2009). These naturally-fertilized regions are exceptional laboratories to study interactions between the Fe and carbon cycling and the role played by microorganisms. The bloom located above the Kerguelen Plateau was investigated in detail during KEOPS1 (Kerguelen Ocean and Plateau compared Study January–February 2005). KEOPS2 (October–November 2011) extended this study to early stages of the bloom and to new investigations in the blooms downstream the island. During KEOPS2 (October–November 2011) we have determined the Fe uptake of the bulk microbial community and of different size-fractions at stations characterized by a wide range of responses to Fe fertilization. We have also conducted a few incubation experiments to specifically study the competition between heterotrophic bacteria and phytoplankton.

2 Materials and methods

2.1 Site description

This study was carried out as part of the KEOPS2 expedition that took place from 9 October to 29 November 2011, in the Indian sector of the Southern Ocean in the vicinity of the Kerguelen archipelago. For the present study 8 stations were sampled (Fig. 1). Station R-2 is the reference station located outside the bloom, west of Kerguelen Island (Fig. 1). The stations E were located in a complex meander south of the Polar Front and sampled in a quasi-Lagrangian manner (D'Ovidio et al., 2014). Characteristics of the stations are given in Table 1.

2.2 Sampling and manipulation under trace metal clean conditions

Seawater samples were collected with 10 L Niskin 1010X-bottles set up on the autonomous Trace Metal Rosette 1018 (TMR) especially adapted for trace metal work

BGD
11, 15053–15086, 2014

(General Oceanics Inc., USA; Bowie et al., 2014). Each Niskin bottle was acid-washed (2 % HCl) and rinsed with milli-Q water before the rosette was deployed for the first time. All metal springs are Teflon coated and the crimps are made of aluminum. All samples were carefully manipulated in a clean container under a laminar flow hood (ISO class 5). Within less than 2 h after sample collection, the seawater was dispersed into 500 mL acid-washed polycarbonate (PC) bottles and the incubations performed as described below. The PC bottles were acid-washed (10 % HCl suprapur, Merck) 3 times, followed by 3 rinses with milliQ-water and they were subsequently sterilized by microwaves (5 min, 750 W). The PC bottles were dried and stored under a laminar flow hood before being used. For the incubation experiments described below, seawater was collected in the surface mixed layer at one depth, and incubated at different levels of surface photosynthetically active radiation (PAR).

2.3 Iron uptake experiments

Three types of incubation experiments were performed (Fig. 2). In one set of experiments, 300 mL of unfiltered seawater were amended with Fe as $^{55}FeCl_3$ (0.2 nM final concentration of ^{55}Fe, specific activity 1.83×10^3 Ci mol^{-1}, Perkin Elmer), incubated for 24 h at 75, 25 and 1 % surface PAR, and then sequentially filtered through 0.8 and 0.2 µm pore size nitrocellulose filters (47 mm diameter, Nuclepore) (Fig. 2a). These incubations, performed at station A3-2, E-4E and E-5, provided measurements of the Fe uptake of the bulk community, based on the sum of the radioactivity measured on the 0.8 and 0.2 µm filters, and of the uptake of Fe by heterotrophic bacteria in the presence of micro-, nano- and picoplankton (> 0.8 µm). In a second set of experiments, seawater (300 mL) was pre-filtered through a 25 µm mesh before 0.2 nM ^{55}Fe was added (final concentration). Following incubation at 75, 45, 25, 16, 4, and 1 % of surface PAR, the seawater was sequentially filtered through 0.8 and 0.2 µm filters (Fig. 2b). The uptake of Fe by pico-nanoplankton (0.8–25 µm), and that of heterotrophic bacteria (0.2–0.8 µm) in the absence of microplankton was derived from these incubations. At the stations where these two types of experiments were performed concurrently

BGD
11, 15053–15086, 2014

(station A3-2, E-4E and E-5), the Fe uptake by microplankton was obtained by the difference between the bulk Fe uptake (Fig. 2a) and the sum of the Fe uptake by pico-nanoplankton and heterotrophic bacteria (Fig. 2b). In a third set of experiments, 300 mL seawater was 0.8 µm pre-filtered prior to the addition of 0.2 nM ^{55}Fe (final concentration). Following the 24 h incubation at 1 % PAR level, the seawater was filtered on a 0.2 µm filter (Fig. 2c). Based on this type of incubation, we determined the Fe uptake by heterotrophic bacteria in the absence of any larger cells. This experiment was performed at stations A3-2, E-4E, E-5, E-4W and R-2. For all the incubations, bottles were maintained at in situ surface temperature in on-deck incubators supplied continuously with surface seawater. The incubators were equipped with Nickel screens simulating light intensities from 75 to 1 %. Incubations were conducted from sunrise to sunrise.

Additionally, to determine if a steady state has been achieved after 24 h of incubation time we performed a separate set of experiments where Fe uptake by bacteria and bacterial cell abundance was followed over 24, 72, 96 h and one week incubation time.

2.4 Determination of intracellular ^{55}Fe

A first step for the assessment of the ^{55}Fe uptake was the removal of ^{55}Fe not incorporated by cells, using a washing solution. Following filtration, the filters were washed with 6 mL of Ti-citrate-EDTA solution (Hudson and Morel, 1989; Tang and Morel, 2006) for 2 min and subsequently rinsed 3 times with 5 mL of 0.2 µm filtered-seawater during 1 min (Fourquez et al., 2012). The filters were placed into plastic vials and 10 mL of the scintillation cocktail Filtercount (Perkin Elmer) was added. Vials were agitated for 24 h before the radioactivity was counted with the Tricarb® scintillation counter. Total radioactivity on filter after correction for background represents intracellular ^{55}Fe. For each station, controls were obtained with 300 mL of microwave-sterilized seawater (750 W for 5 min repeated 3 times) incubated with the same amount of ^{55}Fe and treated in the same way as the live treatments. The radioactivity determined on these filters was considered as background and it is based

BGD
11, 15053–15086, 2014

on the amount of ^{55}Fe adsorbed, but not incorporated by cells. Abiotic adsorption of ^{55}Fe onto cells could be influenced by microwave irradiation if cell structures are altered by the treatment. For technical reasons, we could not use formalin to fix the cells at each station, but we performed a series of tests to compare fixation by formalin and by microwave. The background radioactivity of the formalin-killed seawater was similar to that of the microwave-sterilized seawater, validating our control. We performed one control per station maintained for 24 h at 75 % PAR in the on-deck incubator. The radioactivity measured on the control filters was subtracted from the respective live treatments in all experiments.

To determine the most appropriate concentration of the radioisotope to be added, different amounts of ^{55}Fe were tested: 0.2, 0.4, 1 and 2 nM of unchelated ^{55}Fe (as $^{55}FeCl_3$, final concentrations of ^{55}Fe). We determined that the concentration of 0.2 nM ^{55}Fe was the most appropriate as it minimizes changes in dissolved Fe (DFe) and it still allows detection of the incorporated radioactivity by scintillation counting (for 300 mL of seawater). We also observed that adding more than 0.8 nM of ^{55}Fe (final concentration) stimulates the Fe uptake by microorganisms (pico-nanoplankton and bacteria, data not shown). Using our preferred small addition of 0.2 nM, consumption of ^{55}Fe during our incubations was negligible (1–4 %), with consumption of total dissolved Fe correspondingly even smaller.

The Fe uptake rate (mol Fe L^{-1} d^{-1}) noted ρFe was calculated following the equations:

$$\rho\mathrm{Fe} = \frac{A \cdot {}^{55}\mathrm{Fe\ on\ filter}}{t \cdot V} \quad (1)$$

BGD
11, 15053–15086, 2014

with

$$A = \frac{\text{mol } ^{55}\text{Fe added} + \text{mol DFe in situ}}{\text{mol } ^{55}\text{Fe added}} \quad (2)$$

$$^{55}\text{Fe on filter} = \frac{(\text{cpm on filter sample} - \text{cpm on filter control})}{^{55}\text{Fe specific activity}} \cdot \frac{1}{\text{counting efficiency}} \quad (3)$$

V = volume filtered; t = incubation time; cpm = counts per minute.

2.5 Enumeration of heterotrophic bacteria

Subsamples for cell enumeration were taken at the start and at the end of the incubations. To enumerate heterotrophic bacteria, 2 mL samples were fixed with glutaraldehyde (1 % final concentration), incubated for 1 h at 4 °C, and stored at −80 °C until processed. Heterotrophic bacterial cell abundance was counted with the FASCCanto II BD flow cytometer (Becton, Dickinson). Heterotrophic bacterial cells were stained with SYBRGreen I (Marie et al., 1997) and enumerated for 1 min at a rate of 30 µL min^{-1}. The machine drift was tested using calibration beads (3 µm). Specific bacterial growth rates were calculated from the slope of log-linear regression between the start and the end of the incubation.

2.6 Carbon content of different microbial size-fractions

The cellular carbon content for heterotrophic bacteria was estimated to be 12.4 fg C per cell as reported by Fukuda et al. (1998). The carbon contents for pico-nanoplankton and microplankton were estimated from particulate organic carbon (POC) measured in surface seawater (< 1000 µm) on 300, 210, 50, 20, 5, and 1 µm pore-size filters (see Trull et al., 2014). We assumed the total carbon biomass to be the sum of all these fractions plus the estimated carbon biomass for heterotrophic bacteria. For pico-nanoplankton we assumed the sum of the POC concentrations on the 1 and 5 µm filters,

BGD
11, 15053–15086, 2014

corresponding to the 1–20 µm size-fraction, to be representative of this community. To obtain the carbon biomass for microplankton we subtracted the POC concentration of the 0.2–20 µm size-fraction of the total carbon biomass.

3 Results

3.1 Bulk iron uptake rates and contribution of different size-fractions

The Fe uptake rate (ρFe) for the bulk community, as determined from incubations of unfiltered seawater (Fig. 2a), was measured at stations A3-2, E-4E and E-5, and the volumetric and integrated values are presented on Tables 2 and 3, respectively. The integration of ρFe over the euphotic layer reveals highest values at station E-5 (1.74 µmol Fe m^{-2} d^{-1}), decreasing to 1.12 µmol Fe m^{-2} d^{-1} at station A3-2 and to 0.86 µmol Fe m^{-2} d^{-1} at station E-4E (Table 3). At these three stations the contribution of heterotrophic bacteria to total ρFe was less than 2 % corresponding to a mean integrated uptake of 0.018 ± 0.005 µmol m^{-2} d^{-1} (Table 3). The contribution of the two other size-fractions was station-dependent (Fig. 3). At station E-4E microplankton and pico-nanoplankton had almost equal contributions to total integrated ρFe (53 and 46 %, respectively). At station A3-2 microplankton and pico-nanoplankton accounted for 40 and 59 % of total integrated ρFe, respectively. The contribution of microplankton was the highest at station E-5 (69 % of total integrated ρFe), whereas the contribution of pico-nanoplankton was the lowest (29 % of total integrated ρFe) at this site.

To account for differences in the biomass among stations, we normalized ρFe to the concentration of POC of the microplankton and pico-nanoplankton size-classes and to the estimated cellular carbon content for bacteria, and both ratios are referred to ρFe : POC (Table 2). For the bulk community, a trend similar to ρFe was observed, with the highest ρFe : POC at station E-5 (5.3 ± 1.1 µmol Fe d^{-1} mol C^{-1}; mean±SD of the three PAR levels), decreasing to 3.0 ± 1.0 and 2.5 ± 0.4 µmol Fe d^{-1} mol C^{-1} at stations A3-2 and E-4E, respectively. Because this variability in ρFe : POC could in part reflect

BGD
11, 15053–15086, 2014

differences in ρFe and carbon biomass contribution of organisms, we also considered ρFe : POC for the different size classes. At station E-5 microplankton revealed the highest ρFe : POC ratios (5.25–11.6 µmol Fe d^{-1} mol C^{-1}), while this was the case for pico-nanoplankton at station A3-2 (4.39–7.03 µmol Fe d^{-1} mol C^{-1}). At station E-5, at 75 % of PAR, microplankton revealed the highest ρFe : POC of all measured values. This is driven by the Fe uptake rate because carbon biomass was almost equally partitioned between microplankton (47 % of total carbon biomass) and pico-nanoplankton (44 % of total carbon biomass). Heterotrophic bacterial ρFe : POC was quite homogeneous across depths at stations E-4E (0.49 ± 0.04 µmol Fe d^{-1} mol C^{-1}) and E-5 (0.73 ± 0.07 µmol Fe d^{-1} mol C^{-1}), but it presented high variability at station A3-2, ranging from 0.21 to 1.69 µmol Fe d^{-1} mol C^{-1} (Table 2). As expected, due to the low contribution of heterotrophic bacteria to total ρFe, their carbon-normalized ρFe was the lowest among the three size-fractions.

3.2 Heterotrophic bacterial iron uptake in response to the absence of phytoplankton

To investigate whether heterotrophic bacteria compete with other members of the microbial community for access to Fe, the bacterial Fe uptake rate $(\rho Fe)_{bact}$ and bacterial growth rates were also determined during incubations where microplankton and both microplankton and pico-nanoplankton were excluded (experiments (b) and (c) respectively in Fig. 2). The bacterial uptake rates were denoted $(\rho Fe)_{bact}^{<25\,\mu m}$ if incubated in the absence of microplankton, and $(\rho Fe)_{bact}^{<0.8\,\mu m}$ if incubated in the absence of both microplankton and pico-nanoplankton, while $(\rho Fe : POC)_{bact}$ refers to bacterial Fe uptake rates in the presence of the bulk community. Incubations without microplankton were performed at 6 different light levels. At a given station, the variability of $(\rho Fe)_{bact}^{<25\,\mu m}$ determined at different light levels did not exceed a factor of 4 (Table 4). The unique noticeable exception was station E-3 where $(\rho\ Fe)_{bact}^{<25\,\mu m}$ was about two orders of magnitude higher at 75 % light level. To compare $(\rho Fe)_{bact}^{<25\,\mu m}$ among stations we

BGD
11, 15053–15086, 2014

integrated over the euphotic layer and the mixed layer depths. The outlier value at E-3 (at 75 % PAR level) was not considered for the integration. The lowest depth-integrated values were observed at stations R-2 and E-5 (4.7 nmol Fe m^{-2} d^{-1} at both stations; mean of euphotic and mixed layer integrated fluxes) and the highest values were observed at station E-3 (18.4 nmol Fe m^{-2} d^{-1}). Integrated Fe uptake did not show any clear temporal evolution for the stations at the quasi Lagrangien time series E-2, E-3, E-4E and E-5 (Table 4).

The bacterial Fe uptake rate normalized to cellular carbon content was also determined in the incubations where microplankton was excluded (noted $(\rho\mathrm{Fe}:\mathrm{POC})_{\mathrm{bact}}^{<25\,\mu\mathrm{m}}$ in Table 4). The high value of $(\rho\mathrm{Fe})_{\mathrm{bact}}^{<25\,\mu\mathrm{m}}$ measured at E-3 (at 75 % PAR level) resulted in a high value of $(\rho\mathrm{Fe}:\mathrm{POC})_{\mathrm{bact}}^{<25\,\mu\mathrm{m}}$ (21.4 µmol Fe d^{-1} mol C^{-1}) that is considered as an outlier. All other values ranged from 0.06 to 2.94 µmol Fe d^{-1} mol C^{-1}, and they were 2- to 8-fold lower than those in the corresponding incubations with the bulk community $(\rho\mathrm{Fe}:\mathrm{POC})_{\mathrm{bact}}$ (Stations A3-2, E-4E, and E-5). The normalization does not modify our general observation that there was no significant difference in the rates between the different light levels and between the different stations (two-tailed, unpaired Student's t test, $p = 0.27$). In consideration of this, the values at one given station are now treated as biological replicates.

At the three stations, A3-2, E-4E and E-5 we compared the bacterial Fe uptake in the presence of the whole community $(\rho\mathrm{Fe}:\mathrm{POC})_{\mathrm{bact}}$ with that in the absence of microplankton $(\rho\mathrm{Fe}:\mathrm{POC})_{\mathrm{bact}}^{<25\,\mu\mathrm{m}}$ and that with bacteria alone $(\rho\mathrm{Fe}:\mathrm{POC})_{\mathrm{bact}}^{<0.8\,\mu\mathrm{m}}$ (Fig. 4). For all stations, we found that bacterial Fe uptake was the highest in the absence of any other larger cells and the lowest in absence of microplankton with $(\rho\mathrm{Fe}:\mathrm{POC})_{\mathrm{bact}}^{<0.8\,\mu\mathrm{m}} > (\rho\mathrm{Fe}:\mathrm{POC})_{\mathrm{bact}} > (\rho\mathrm{Fe}:\mathrm{POC})_{\mathrm{bact}}^{<25\,\mu\mathrm{m}}$. When bacteria where incubated with the entire microbial community, $(\rho\mathrm{Fe}:\mathrm{POC})_{\mathrm{bact}}$ was 2 to 8.5 times higher than in the incubations without microplankton ($(\rho\mathrm{Fe}:\mathrm{POC})_{\mathrm{bact}}^{<25\,\mu\mathrm{m}}$), but still lower than when bacteria were incubated alone. Similarly to $(\rho\mathrm{Fe}:\mathrm{POC})_{\mathrm{bact}}^{<0.8\,\mu\mathrm{m}}$, bacterial growth

BGD
11, 15053–15086, 2014

rates increased by 2 to 5 times when bacteria were incubated alone compared to incubations where microplankton were absent (Fig. 4b).

3.3 Growth rates and iron quota of heterotrophic bacteria

In the experiments where micro-, pico- and nanoplankton were absent (Fig. 2c) the abundance of heterotrophic bacteria was determined at the beginning and at the end of the incubation period. Assuming an exponential growth during the incubation provided an estimate of the growth rates. The lowest growth rate ($0.02\,d^{-1}$) was determined at the station R-2. For the other stations, the growth rate ranged from $0.12 d^{-1}$ (E-5) to $0.36 d^{-1}$ (E-3). We also measured $(\rho Fe : POC)^{<0.8\,\mu m}_{bact}$ after 24, 72, 96 h and after 7 days of incubation. The $(\rho Fe : POC)^{<0.8\,\mu m}_{bact}$ was similar after 24 and 96 h of incubation and decreased after one week of incubation (data not shown). This suggests that 24 h of incubation provides a measurement of steady state Fe uptake rate. Thus, we derived the Fe quota for heterotrophic bacteria (Q_{Fe}) based on the equation $\rho = \mu Q_{Fe}$ (Fig. 5). The Fe quota of heterotrophic bacteria was 4×10^{-20} mol Fe cell^{-1} for stations R-2, E-5, and E-4W, and 8×10^{-20} mol Fe cell^{-1} for station E-2, F-L, A3-2 and E-3.

4 Discussion

4.1 The microbial Fe demand

In the vicinity of the Kerguelen Islands, natural Fe fertilization produces many blooms with different dynamics resulting from a combination of hydrodynamic and ecological drivers. These sites provide excellent opportunities to investigate the demand of different members of the microbial community for Fe, and how these members interact. During the project KEOPS2 we visited a variety of early spring blooms located above the Kerguelen plateau and in offshore waters north and south of the Polar Front. We

BGD
11, 15053–15086, 2014

start our discussion by putting our results in the context of previous studies related to Fe uptake by the microbial community in the Southern Ocean.

In the early spring bloom located above the Kerguelen Plateau (station A3-2), the total Fe demand, defined here as the steady state Fe uptake rate by the bulk community, was 33.2 pmol Fe L^{-1} d^{-1} in surface. This Fe demand is more than 6 times higher than that determined during KEOPS1 at the same site during the declining phase of the bloom (5.3 ± 1.2 pmol L^{-1} d^{-1} for a mean value of A3-4 and A3-5, 50 % PAR, Sarthou et al., 2008). The Fe demand during KEOPS2 is also higher than that measured during the artificial Fe fertilization experiment SOIREE in Antarctic zone. At about 13 days following the Fe addition, a time-point which corresponded to the growing phase of the bloom, Bowie et al. (2001) determined an Fe demand of 11.9 pmol L^{-1} d^{-1} (mean mixed layer). The differences in the Fe demand between these three studies likely do not result from differences in biomass, because POC concentrations in the surface mixed layer were similar between studies (10–12 µM; Bowie et al., 2001; Sarthou et al., 2008; Trull et al., 2014).

For the KEOPS expeditions, different stages of the bloom provide a temporal framework to interpret these observations. However, this is not the case for the differences observed between KEOPS2 and SOIREE, which were both sampled during the early phase of a bloom, even if the blooms occurred at different seasons. Besides the seasonal differences, the location of the study could explain the variability in the Fe demand. Finally, the results of FeCycle provide a comparison with the Sub Antarctic zone. The Fe demand determined for the steady-state microbial Fe budget was 26–101 pmol L^{-1} d^{-1} (Strzepek et al., 2005), thus at the upper bound or higher than during KEOPS2, although carbon biomasses were similar (10.2 µM, average for the mixed layer). From all these comparisons it appears that besides the variability driven by temporal or spatial factors, a plankton-based mechanistic explanation is certainly required for a better understanding of the observed differences.

Culture studies (Sunda and Huntsman, 1997; Strzepek and Harrison, 2004; Marchetti et al., 2009) or molecular approaches (Allen et al., 2008) have shown

BGD
11, 15053–15086, 2014

that there are multiple strategies for phytoplankton to deal with Fe limitation. The consequences are that bulk cell properties like the Fe uptake rate, the intracellular Fe concentration or the elemental Fe : C ratio are species dependent. However, the use of this basic knowledge to interpret field results is not straightforward. This is primarily due to the complexity of the natural phytoplankton community, but it is also obscured by possible regional differences as shown by Strzepek et al. (2012). Southern Ocean phytoplankton species responded to Fe-light acclimation differently than temperate species (Sunda and Huntsman, 1997; Strzepek et al., 2012). In the case of heterotrophic bacteria, culture studies (Granger and Price, 1999; Armstrong et al., 2004; Fourquez et al., 2014) and metagenomic analysis (Hopkinson and Barbeau, 2012; Toulza et al., 2012) have also provided foundations for our understanding of the responses of bacteria to Fe limitation but extrapolation to field observations face the same constraints as mentioned for phytoplankton.

A first step forward, even if not perfect, to obtain some insight into the role of the community composition is to compare parameters in different size-fractions. In Fe-fertilized systems, the largest size-fraction (> 25 µm), named microplankton is almost entirely composed of diatoms. In the early spring bloom above the Kerguelen plateau, this fraction contributed 40 % of the total Fe uptake. This is substantially lower than during the declining phase of the bloom where 62 % of total Fe uptake was accounted for by microplankton (Sarthou et al., 2008). This decrease in the contribution of microplankton is consistent with the idea that the early phase of the bloom is dominated by a succession of rapidly growing diatoms of different sizes, and that larger slow growing, and silicon limited diatoms accumulate at the end of the season (Quéguiner, 2013). At the onset of the bloom above the plateau, pico-nanoplankton were the main contributor to Fe uptake (69 %) and this size-fraction also revealed the highest carbon-normalized Fe uptake rates. This fraction contains mainly small diatoms because non-diatom phytoplankton, as determined by flow cytometry, represented about 10 % of the POC in this size-fraction at station A3-2 (7.4 ± 0.4, $n = 6$). This suggests that the diatoms belonging to this size class are more competitive than larger cells for the

BGD
11, 15053–15086, 2014

conditions prevailing at this period of the season. The same observation holds for the FeCycle experiment in the Sub-Antarctic where the Fe uptake was dominated by photosynthetic pico-nanoplankton during the early bloom (Strzepek et al., 2005; Boyd and Ellwood, 2010).

In addition to ρFe : POC, we have also calculated the Fe : C uptake ratios based on in situ primary production measurements (Cavagna et al., this issue). In the Southern Ocean, Fe : C uptake ratios (noted ρFe : ρC) reported in the literature range from $\sim$ 5 to 50 µmol Fe mol C^{-1} and can reach up to 100 µmol Fe mol C^{-1}, as it was reported in some artificial Fe fertilizations (Boyd et al., 2000). During KEOPS2, the ρFe : ρC ranged from 3.7 (station A3-2) to 22.9 µmol Fe mol C^{-1} (station E-5, Fig. 6). The values determined for the plateau station A3-2 (3.7–11 µmol Fe mol C^{-1}) are similar to those reported for the declining phase of the bloom during KEOPS1 (5.0 ± 2.6 µmol Fe mol C^{-1}, average for stations A3-1, A3-4, and A3-5 (Sarthou et al., 2008). These Fe : C uptake ratios are also consistent with values measured during the two FeCycle studies where ρFe : ρC were comprised between 5.5 and 19 µmol Fe mol C^{-1}, and did not vary much with depth and over time (Strzepek et al., 2005; King et al., 2012). By contrast, at the stations located downstream the plateau (E-4E and E-5) the ρFe : ρC values were overall higher than above the plateau (range from 10 to 22 µmol Fe mol C^{-1}).

So, while ρFe : POC ratios during the early bloom were much higher than during the late bloom, the ρFe : ρC ratios during KEOPS2 are similar to KEOPS1. Changes in phytoplankton community composition and physiological state over time (Armand et al., 2008; Quéguiner, 2013; Lasbleiz et al., 2014) could have a stronger effect on carbon normalized Fe uptake than on the ratio Fe uptake: primary production.

4.2 Phytoplankton-bacteria competition for iron acquisition

During KEOPS2, heterotrophic bacteria contributed less than 2 % to the total Fe uptake (ρFe). This is similar to the low contribution of heterotrophic bacteria of 1 to 5 % to the total ρFe during FeCycle (Strzepek et al., 2005), but contrasts with observations from

BGD
11, 15053–15086, 2014

the subarctic Pacific where heterotrophic bacteria dominated the Fe uptake (20–45 %, Tortell et al., 1996).

Heterotrophic bacterial Fe uptake was negatively affected by the presence of pico- to microplankton, suggesting competition between these members of the microbial community. Competition for the limiting nutrient is not unexpected, however, this issue has rarely been addressed in previous studies (Boyd, 2012). Bacterial and pico-nanoplanktonic cells could compete for nutrients as both have comparable metabolic rates (Massana and Logares, 2012), and high capacities for resource acquisition. Our observation of the overall low contribution of heterotrophic bacteria to bulk Fe uptake suggests that not only the access to Fe, but also organic carbon could have limited the bacterial response to natural fertilization. This idea is supported by the relation between the extent of stimulation of bacterial Fe uptake in fertilized waters and the increase in primary production (Fig. 7).

The bacterial Fe uptake rates were highest when measured in the absence of any larger cells and the lowest when in the absence of microplankton only (Fig. 4a). This is verified for all stations where the experiment was conducted, except for the reference station R-2 where no differences in bacterial Fe uptake rates between these treatments were detectable. This strongly suggests that for the stations located in Fe-fertilized regions, phytoplankton, and in particular pico-nanoplankton, competed with bacteria for Fe acquisition. Assuming that the increase in phytoplankton activity results in an increase in bacterial Fe-limitation, primary production and bacterial Fe uptake should be negatively correlated. In fact $(\rho\mathrm{Fe}:\mathrm{POC})_{\mathrm{bact}}^{<25\,\mu\mathrm{m}}$ and primary production are weakly positively correlated (Fig. 7a). This can be explained if the negative effect due to the competition with phytoplankton for Fe was masked by the positive effect due to the stimulation of bacteria by enhanced primary production due to dissolved organic carbon (DOC) availability. This idea is supported by the high positive correlation between $(\rho\mathrm{Fe}:\mathrm{POC})_{\mathrm{bact}}^{<0.8\,\mu\mathrm{m}}$ and primary production (Fig. 7b). We propose two non-exclusive explanations for the observed positive correlation between these two parameters. First, the increase in primary production could be

BGD
11, 15053–15086, 2014

driven by an increase in Fe availability that may also benefit to heterotrophic bacteria when competition with larger cells is alleviated. Second, the increase in primary production could result in an enhanced amount of phytoplankton-derived DOC, which in turn stimulates the bacterial Fe demand. Both mechanisms are likely to occur, as independent experiments during KEOPS2 revealed that bacterial production was stimulated by both, and single additions of Fe and organic carbon (Obernosterer et al., 2014). DOC is undoubtedly one of the most important substrates provided by autotrophic phytoplankton cells to heterotrophic bacteria. The amount of DOC produced by phytoplankton during the bloom is likely to play in Fe demand by bacteria. Kirchman et al. (2000) suggested that low Fe availability leads to increase the C demand and more recently, Fourquez et al. (2014) have provided some evidence that marine heterotrophic bacteria reallocate their inner resources to sustain this increase of the C demand when Fe limited. Here, we also show that high C availability leads to an increase in Fe demand. Finally we note that the minimum values of $(\rho\mathrm{Fe}:\mathrm{POC})_{\mathrm{bact}}^{<25\,\mu\mathrm{m}}$ in comparison to whole community $(\rho\mathrm{Fe}:\mathrm{POC})_{\mathrm{bact}}$ and bacteria-only $(\rho\mathrm{Fe}:\mathrm{POC})_{\mathrm{bact}}^{<0.8\,\mu\mathrm{m}}$ incubations could arise via other microorganism allelopathic interaction mechanisms than competition for Fe. As such, further research is needed to examine interactions between pico-nanoplankton and bacteria across a wider range of conditions, i.e. including non-limiting Fe and carbon substrate levels.

Our observation that small diatoms were particularly competitive in removing Fe during the early stage of the spring phytoplankton bloom induced by natural Fe-fertilization in the Southern Ocean suggests an intimate connection between heterotrophic bacteria and pico-nanoplankton. If this is the case, a progressive shift in the community composition from small to larger diatoms in the course of a bloom (Quéguiner, 2013) would affect the bacterial Fe uptake rates over time. This could partly explain why heterotrophic bacteria accounted for 17–27 % of the overall Fe-uptake at the late stage of the spring bloom (Sarthou et al., 2008) in contrast to 1–2 % at the onset of the bloom. Together, these results demonstrate that the bacterial Fe and carbon

BGD
11, 15053–15086, 2014

metabolism are closely coupled, and that the structure of the microbial community has a marked effect on the extent of bacterially-mediated Fe cycling.

Acknowledgements. We would like to thanks the captain Bernard Lassiette, the chief scientist Bernard Quéguiner, and the crew of the R/V *Marion-Dufresne II* for assistance on board. We are also grateful to Laurent Besnard for his assistance in creating Fig. 1. This work was supported by the French Research program of INSU-CNRS LEFE-CYBER (Les enveloppes fluides et l'environnement – Cycles biogéochimiques, environnement et ressources), the French ANR (Agence Nationale de la Recherche, SIMI-6 program, ANR-10-BLAN-0614), the French CNES (Centre National d'Etudes Spatiales) and the French Polar Institute IPEV (Institut Polaire Paul-Emile Victor).

References

Allen, A. E., Laroche, J., Maheswari, U., Lommer, M., Schauer, N., Lopez, P. J., Finazzi, G., Fernie, A. R., and Bowler, C.: Whole-cell response of the pennate diatom Phaeodactylum tricornutum to iron starvation, P. Natl. Acad. Sci. USA, 105, 10438–10443, 2008.

Amin, S. A., Green, D. H., Hart, M. C., Küpper, F. C., Sunda, W. G., Carrano, C. J., and Ku, F. C.: Photolysis of iron – siderophore chelates promotes bacterial – algal mutualism, P. Natl. Acad. Sci. USA, 106, 17071–17076, 2009.

Armand, L. K., Cornet-Barthaux, V., Mosseri, J., and Quéguiner, B.: Late summer diatom biomass and community structure on and around the naturally iron-fertilised Kerguelen Plateau in the Southern Ocean, Deep-Sea Res. Pt. II, 55, 653–676, 2008.

Armstrong, E., Granger, J., Mann, E. L., and Price, N. M.: Outer-membrane siderophore receptors of heterotrophic oceanic bacteria, Limnol. Oceanogr., 49, 579–587, 2004.

Arrigo, K. R.: Molecular diversity and ecology of microbial plankton, Nature, 437, 343–348, 2005.

Blain, S., Quéguiner, B., Armand, L., Belviso, S., Bombled, B., Bopp, L., Bowie, A., Brunet, C., Brussaard, C., Carlotti, F., Christaki, U., Corbière, A., Durand, I., Ebersbach, F., Fuda, J.-L., Garcia, N., Gerringa, L., Griffiths, B., Guigue, C., Guillerm, C., Jacquet, S., Jeandel, C., Laan, P., Lefèvre, D., Lo Monaco, C., Malits, A., Mosseri, J., Obernosterer, I., Park, Y.-H., Picheral, M., Pondaven, P., Remenyi, T., Sandroni, V., Sarthou, G., Savoye, N., Scouarnec, L., Souhaut, M., Thuiller, D., Timmermans, K., Trull, T., Uitz, J., van Beek, P.,

BGD
11, 15053–15086, 2014

Veldhuis, M., Vincent, D., Viollier, E., Vong, L., and Wagener, T.: Effect of natural iron fertilization on carbon sequestration in the Southern Ocean., Nature, 446, 1070–1074, 2007.
Blain, S., Capparos, J., Guéneuguès, A., Obernosterer, I., and Oriol, L.: Distributions and stoichiometry of dissolved nitrogen and phosphorus in the iron fertilized region near Kerguelen (Southern Ocean), Biogeosciences Discuss., 11, 9949–9977, doi:10.5194/bgd-11-9949-2014, 2014.
Bowie, A. R., Maldonado, M. T., Frew, R. D., Croot, P. L., Achterberg, E. P., Mantoura, R. F. C., Worsfold, P. J., Law, C. S., and Boyd, P. W.: The fate of added iron during a mesoscale fertilisation experiment in the Southern Ocean, Deep-Sea Res. Pt. II, 48, 2703–2743, 2001.
Bowie, A. R., van der Merwe, P., Trull, T. W., Quéroué, F., Fourquez, M., Planchon, F., Sarthou, G., and Blain, S.: Iron budgets for three distinct biogeochemical sites around the Kerguelen plateau (Southern Ocean) during the natural fertilization experiment KEOPS-2, Biogeosciences Discuss., submitted, 2014.
Boyd, P. W. and Ellwood, M. J.: The biogeochemical cycle of iron in the ocean, Nat. Geosci., 3, 675–682, 2010.
Boyd, P. W., Watson, A. J., Law, C. S., Abraham, E. R., Trull, T., Murdoch, R., Bakker, D. C., Bowie, A. R., Buesseler, K. O., Chang, H., Charette, M., Croot, P., Downing, K., Frew, R., Gall, M., Hadfield, M., Hall, J., Harvey, M., Jameson, G., LaRoche, J., Liddicoat, M., Ling, R., Maldonado, M. T., McKay, R. M., Nodder, S., Pickmere, S., Pridmore, R., Rintoul, S., Safi, K., Sutton, P., Strzepek, R. F., Tanneberger, K., Turner, S., Waite, A., and Zeldis, J.: A mesoscale phytoplankton bloom in the polar Southern Ocean stimulated by iron fertilization, Nature, 315, 612–617, 2000.
Boyd, P. W., Strzepek, R., Chiswell, S., Chang, H., DeBruyn, J. M., Ellwood, M., Keenan, S., King, A. L., Maas, E. W., Nodder, S., Sander, S. G., Sutton, P., Twining, B. S., Wilhelm, S. W., and Hutchins, D. A.: Microbial control of diatom bloom dynamics in the open ocean, Geophys. Res. Lett., 39, 1–6, 2012.
Closset, I., Lasbleiz, M., Leblanc, K., Quéguiner, B., Cavagna, A.-J., Elskens, M., Navez, J., and Cardinal, D.: Seasonal evolution of net and regenerated silica production around a natural Fe-fertilized area in the Southern Ocean estimated with Si isotopic approaches, Biogeosciences, 11, 5827–5846, doi:10.5194/bg-11-5827-2014, 2014.
d'Ovidio, F., Nencioli, F., Pujol, I., Rio, M. H., Park, Y.-H., Queguiner, B., and Blain, S.: The multisatellite-based adaptive strategy of the KEOPS2 cruise, Report to Cospar, 84–85, 2014

BGD
11, 15053–15086, 2014

Fourquez, M., Obernosterer, I., and Blain, S.: A method for the use of the radiotracer 55Fe for microautoradiography and CARD-FISH of natural bacterial communities, FEMS Microbiol. Lett., 337, 132–139, 2012.
Fourquez, M., Devez, A., Schaumann, A., Guéneuguès, A., Jouenne, T., Obernosterer, I., and Blain, S.: Effects of iron limitation on growth and carbon metabolism in oceanic and coastal heterotrophic bacteria, Limnol. Oceanogr., 59, 349–360, 2014.
Fukuda, R., Ogawa, H., Nagata, T., and Koike, I.: Direct determination of carbon and nitrogen contents of natural bacterial assemblages in marine environments, Appl. Environ. Microb., 64, 3352–3358, 1998.
Granger, J. and Price, N. M.: The importance of siderophores in iron nutrition of heterotrophic marine bacteria, Limnol. Oceanogr., 44, 541–555, 1999.
Hassler, C. S., Alasonati, E., Mancuso Nichols, C. A., and Slaveykova, V. I.: Exopolysaccharides produced by bacteria isolated from the pelagic Southern Ocean – Role in Fe binding, chemical reactivity, and bioavailability, Mar. Chem., 123, 88–98, 2011a.
Hassler, C. S., Schoemann, V., Nichols, C. M., Butler, E. C. V., and Boyd, P. W.: Saccharides enhance iron bioavailability to Southern Ocean phytoplankton, Proc. Natl. Acad. Sci. USA, 108, 1076–1081, 2011b.
Hopkinson, B. M. and Barbeau, K. A.: Iron transporters in marine prokaryotic genomes and metagenomes, Environ. Microbiol., 14, 114–28, 2012.
Hudson, R. J. M. and Morel, F. M. M.: Distinguishing between extra- and intracellular iron in marine phytoplankton, Limnol. Oceanogr., 34, 1113–1120, 1989.
King, A. L., Sañudo-Wilhelmy, S. A., Boyd, P. W., Twining, B. S., Wilhelm, S. W., Breene, C., Ellwood, M. J., and Hutchins, D. A.: A comparison of biogenic iron quotas during a diatom spring bloom using multiple approaches, Biogeosciences, 9, 667–687, doi:10.5194/bg-9-667-2012, 2012.
Kirchman, D. L., Meon, B., Cottrell, M. T., Hutchins, D. A., Weeks, D., and Bruland, K. W.: Carbon versus iron limitation of bacterial growth in the California upwelling regime, Limnol. Oceanogr., 45, 1681–1688, 2000.
Lasbleiz, M., Leblanc, K., Blain, S., Ras, J., Cornet-Barthaux, V., Hélias Nunige, S., and Quéguiner, B.: Pigments, elemental composition (C, N, P, Si) and stoichiometry of particulate matter, in the naturally iron fertilized region of Kerguelen in the Southern Ocean, Biogeosciences Discuss., 11, 8259–8324, doi:10.5194/bgd-11-8259-2014, 2014.

BGD
11, 15053–15086, 2014

Litchman, E., Klausmeier, C. A., and Bossard, P.: Phytoplankton nutrient competition under dynamic light regimes, Limnol. Oceanogr., 49, 1457–1462, 2004.
Madsen, E. L.: Microorganisms and their roles in fundamental biogeochemical cycles, Curr. Opin. Biotech., 22, 456–64, 2011.
Maldonado, M. T., Boyd, P. W., LaRoche, J., Strzepek, R. F., Waite, A., Bowie, A. R., Croot, P. L., Frew, R. D., and Price, N. M.: Iron uptake and physiological response of phytoplankton during a mesoscale Southern Ocean iron enrichment, Limnol. Oceanogr., 46, 1802–1808, 2001.
Marchetti, A., Parker, M. S., Moccia, L. P., Lin, E. O., Arrieta, A. L., Ribalet, F., Murphy, M. E. P., Maldonado, M. T., and Armbrust, E. V.: Ferritin is used for iron storage in bloom-forming marine pennate diatoms, Nature, 457, 467–470, 2009.
Marie, D., Partensky, F., Jacquet, S., and Vaulot, D.: Enumeration and cell cycle analysis of natural populations of marine picoplankton by flow cytometry using the nucleic acid stain SYBR Green I, Appl. Environ. Microb., 63, 186–193, 1997.
Massana, R. and Logares, R.: Eukaryotic versus prokaryotic marine picoplankton ecology, Environ. Microbiol., 15, 1254–1261, 2012.
Mills, M. M., Moore, C. M., Langlois, R., Milne, A., Achterberg, E. P., Nachtigall, K., Lochte, K., Geider, R. J., and La Roche, J.: Nitrogen and phosphorus co-limitation of bacterial productivity and growth in the oligotrophic subtropical North Atlantic, Limnol. Oceanogr., 53, 824–834, 2008.
Obernosterer, I., Fourquez, M., and Blain, S.: Fe and C co-limitation of heterotrophic bacteria in the naturally fertilized region off Kerguelen Islands, Biogeosciences Discuss., submitted, 2014.
Pollard, R. T., Salter, I., Sanders, R. J., Lucas, M. I., Moore, C. M., Mills, R. A., Statham, P. J., Allen, J. T., Baker, A. R., Bakker, D. C. E., Charette, M. A., Fielding, S., Fones, G. R., French, M., Hickman, A. E., Holland, R. J., Hughes, J. A., Jickells, T. D., Lampitt, R. S., Morris, P. J., Nédélec, F. H., Nielsdóttir, M., Planquette, H., Popova, E. E., Poulton, A. J., Read, J. F., Seeyave, S., Smith, T., Stinchcombe, M., Taylor, S., Thomalla, S., Venables, H. J., Williamson, R., and Zubkov, M. V.: southern Ocean deep-water carbon export enhanced by natural iron fertilization, Nature, 457, 577–580, 2009.
Quéguiner, B.: Iron fertilization and the structure of planktonic communities in high nutrient regions of the Southern Ocean, Deep-Sea Res. Pt. II, 90, 43–54, 2013.

BGD
11, 15053–15086, 2014

Sarthou, G., Vincent, D., Christaki, U., Obernosterer, I., Timmermans, K. R., and Brussaard, C. P. D.: The fate of biogenic iron during a phytoplankton bloom induced by natural fertilisation: impact of copepod grazing, Deep-Sea Res. Pt. II, 55, 734–751, 2008.

Strzepek, R. F. and Harrison, P. J.: Photosynthetic architecture differs in coastal and oceanic diatoms, Nature, 403, 689–692, 2004.

Strzepek, R. F., Hunter, K. A., Frew, R. D., Harrison, P. J., and Boyd, P. W.: Iron-light interactions differ in Southern Ocean phytoplankton, Limnol. Oceanogr., 57, 1182–1200, 2012.

Strzepek, R. F., Maldonado, M. T., Higgins, J. L., Hall, J., Safi, K., Wilhelm, S. W., and Boyd, P. W.: Spinning the "Ferrous Wheel": the importance of the microbial community in an iron budget during the FeCycle experiment, Global Biogeochem. Cy., 19, 1–14, 2005.

Sunda, W. G. and Huntsman, S. A.: Interrelated influence of iron, light and cell size on marine phytoplankton growth, Nature, 390, 389–392, 1997.

Tang, D. and Morel, F. M. M.: Distinguishing between cellular and Fe-oxide-associated trace elements in phytoplankton, Mar. Chem., 98, 18–30, 2006.

Tortell, P. D., Maldonado, M. T., and Price, N. M.: The role of heterotrophic bacteria in iron-limited ocean ecosystems, Nature, 383, 330–332, 1996.

Toulza, E., Tagliabue, A., Blain, S., and Piganeau, G.: Analysis of the global ocean sampling (GOS) project for trends in iron uptake by surface ocean microbes, edited by: Rodriguez-Valera, F., PLoS One, 7, e30931, doi:10.1371/journal.pone.0030931, 2012.

BGD
11, 15053–15086, 2014

Table 1. Location, date, depth of sampling and mean biogeochemical properties from studied stations.

Station	Latitude S	Longitude E	Date of sampling (dd/mm/yyyy)	Depth of sampling (m)	SST (°C)	$NO_3^- + NO_2^-$ [a] (µmol L^{-1})	PO_4^{3-} [a] (µmol L^{-1})	$Si(OH)_4$ [b] (µmol L^{-1})	Chla [c] (µg L^{-1})	DFe [d] (nmol L^{-1})	Experimental approach [e]
HNLC reference											
R-2	−50.3590	66.7170	26/10/2011	40	2.3	25.4	1.81	12.1	0.32	0.09	b, c
Kerguelen plateau											
A3-2	−50.6240	72.0560	17/11/2011	20	2.3	25.2	1.75	18.4	1.6	0.18	a, b, c
Polar Front											
F-L	−48.5320	74.6590	07/11/2011	20	4.3	18.5	0.900	6.45	2.8	0.26	b
Downstream plume											
E-2	−48.5230	72.0770	01/11/2011	20	3.0	26.6	1.74	14.5	0.42	0.08	b
E-3	−48.7020	71.9670	02/11/2011	20	3.1	25.4	1.78	15.1	0.079	0.38	b
E-4W	−48.7650	71.4250	12/11/2011	20	2.7	25.3	1.74	17.5	0.56	0.20	b, c
E-4E	−48.7150	72.5630	13/11/2011	20	3.2	24.3	1.62	12.1	1.3	0.19	a, b, c
E-5	−48.4120	71.9000	19/11/2011	20	3.3	25.0	1.73	11.5	1.1	0.06	a, b, c

[a] From Blain et al. (2014),
[b] From Closset et al. (2014),
[c] From Lasbleiz et al. (2014),
[d] From Quéroué et al. (2014),
[e] see for details Fig. 2 and Sect. 2.3.

BGD
11, 15053–15086, 2014

Table 2. Iron uptake rates and C-normalized Fe uptake rates of the bulk community and the three size-fractions for incubations conducted at 75, 25 and 1 % of the photosynthetically active radiation (PAR) on unfiltered seawater (see text and Fig. 2a for details).

Station	PAR (%)	Fe uptake rate (pmol Fe d^{-1} L^{-1})				C-normalized Fe uptake rate (µmol Fe d^{-1} mol C^{-1})			
		Bulk community (> 0.2µm)	Microplankton (> 25µm)	Pico-nanoplankton (0.8–25 µm)	Heterotrophic bacteria (0.2–0.8 µm)	Total*	Microplankton (> 25µm)	Pico-nanoplankton (0.8–25 µm)	Heterotrophic bacteria (0.2–0.8 µm)
A3-2	75	33.2	15.5	17.7	0.07	3.26	2.25	5.84	0.21
	25	19.0	5.1	13.3	0.60	1.86	0.75	4.39	1.69
	1	39.8	17.9	21.3	0.57	3.87	2.60	7.03	1.37
E-4E	75	28.1	13.4	14.3	0.30	2.78	2.50	1.19	0.45
	25	26.5	13.2	12.8	0.43	2.56	2.47	1.07	0.52
	1	22.6	13.5	8.8	0.34	2.03	2.52	0.73	0.49
E-5	75	39.5	33.7	5.3	0.46	6.33	11.6	1.93	0.80
	25	32.7	22.4	9.9	0.41	5.27	7.68	3.61	0.73
	1	26.3	15.3	1.1	0.39	4.23	5.25	0.39	0.66

* Total ρFe : POC was calculated as the sum of the Fe uptake rates of the three size-fractions divided by the sum of particulate organic carbon of each size-fraction.

BGD
11, 15053–15086, 2014

Table 3. Euphotic layer integrated Fe uptake of the bulk community and three size-fractions. The depth of the euphotic layer is 39 m for A3-2, 80 m for E-4E and 41 m for E-5.

Station	Euphotic layer integrated Fe uptake (µmol Fe m^{-2} d^{-1})			
	Bulk community (> 0.2 µm)	Microplankton (> 25µm)	Pico-nanoplankton (0.8–25 µm)	Heterotrophic bacteria (0.2–0.8 µm)
A3-2	1.12	0.44	0.66	0.019
E-4E	0.86	0.45	0.40	0.013
E-5	1.74	1.21	0.51	0.023

BGD
11, 15053–15086, 2014

Table 4. Bacterial carbon biomass (particulate organic carbon, POC), bacterial Fe uptake rates, C-normalized Fe uptake rates, and integrated Fe uptake (to the euphotic layer depth, Ze; to the mixed layer depth, MLD; average, avg). Values given in the columns $(POC)_{bact}^{<25\mu m}$, $(\rho Fe)_{bact}^{<25\mu m}$, and $(\rho Fe : POC)_{bact}^{<25\mu m}$ are relative to incubations conducted in the absence of microplankton. Values given in the columns $(POC)_{bact}$, $(\rho Fe)_{bact}$, and $(\rho Fe : POC)_{bact}$ are relative to incubation performed with the bulk community. Integrated values are calculated from incubations in absence of microplankton. n.d: no data available.

Station	PAR level	Biomass (POC) ($\mu g\,C\,L^{-1}$)		Fe uptake rate ($pmol\,Fe\,L^{-1}\,d^{-1}$)		C-normalized Fe uptake rate ($\mu mol\,Fe\,d^{-1}\,mol\,C^{-1}$)		Integrated Fe ($nmol\,Fe\,m^{-2}\,d^{-1}$)		
		$(POC)_{bact}^{<25\mu m}$	$(POC)_{bact}$	$(\rho Fe)_{bact}^{<25\mu m}$	$(\rho Fe)_{bact}$	$(\rho Fe : POC)_{bact}^{<25\mu m}$	$(\rho Fe : POC)_{bact}$	Ze	MLD	avg
E-4E	75 %	13.4	8.05	0.10	0.30	0.09	0.45	9.7	12.8	11.3
	45 %	8.36	n.d	0.19	n.d	0.28	n.d			
	25 %	7.30	9.86	0.16	0.43	0.26	0.52			
	16 %	8.54	n.d	0.40	n.d	0.56	n.d			
	4 %	9.67	n.d	0.23	n.d	0.28	n.d			
	1 %	8.77	8.35	0.17	0.34	0.23	0.49			
A3-2	75 %	n.d	4.34	0.25	0.07	n.d	0.21	6.6	13.1	9.9
	45 %	4.36	n.d	0.19	n.d	0.51	n.d			
	25 %	4.65	4.28	0.10	0.60	0.26	1.69			
	16 %	4.46	n.d	0.11	n.d	0.30	n.d			
	4 %	7.92	n.d	0.18	n.d	0.27	n.d			
	1 %	4.69	4.97	0.16	0.57	0.40	1.37			
E-5	75 %	6.56	6.93	0.05	0.46	0.10	0.80	5.2	4.2	4.7
	45 %	6.88	n.d	0.06	n.d	0.10	n.d			
	25 %	6.42	6.68	0.07	0.41	0.13	0.73			
	16 %	6.76	n.d	0.06	n.d	0.11	n.d			
	4 %	8.26	n.d	0.13	n.d	0.19	n.d			
	1 %	6.42	7.12	0.14	0.39	0.27	0.66			
R-2	75 %	3.52		0.07		0.23		4.4	5.0	4.7
	45 %	3.16		0.04		0.14				
	25 %	n.d	n.d	0.29	n.d	n.d	n.d			
	16 %	3.60		0.25		0.82				
	4 %	3.53		0.05		0.16				
	1 %	3.29		0.05		0.19				

BGD
11, 15053–15086, 2014

Table 4. Continued.

Station	PAR level	Biomass (POC) ($\mu g\,C\,L^{-1}$)		Fe uptake rate ($pmol\,Fe\,L^{-1}\,d^{-1}$)		C-normalized Fe uptake rate ($\mu mol\,Fe\,d^{-1}\,mol\,C^{-1}$)		Integrated Fe ($nmol\,Fe\,m^{-2}\,d^{-1}$)		
		$(POC)^{<25\mu m}_{bact}$	$(POC)_{bact}$	$(\rho Fe)^{<25\mu m}_{bact}$	$(\rho Fe)_{bact}$	$(\rho Fe:POC)^{<25\mu m}_{bact}$	$(\rho Fe:POC)_{bact}$	Ze	MLD	avg
E-2	75 %	5.33	n.d	0.07	n.d	0.16	n.d	5.8	5.8	5.8
	45 %	6.00		0.05		0.09				
	25 %	6.80		0.06		0.11				
	16 %	n.d		0.27		n.d				
	4 %	7.04		0.05		0.09				
	1 %	6.60		0.00		0.06				
E-3	75 %	8.66	n.d	15.50	n.d	21.4	n.d	20.0*	16.8*	18.4*
	45 %	7.23		0.25		0.41				
	25 %	9.73		0.41		0.51				
	16 %	8.63		0.25		0.35				
	4 %	10.53		0.32		0.36				
	1 %	9.01		0.29		0.39				
F-L	75 %	6.49	n.d	0.84	n.d	1.56	n.d	14.0	18.4	16.2
	45 %	9.67		0.36		0.45				
	25 %	9.67		0.58		0.72				
	16 %	1.02		0.25		2.94				
	4 %	4.74		0.50		1.26				
	1 %	27.7		0.49		0.21				
E-4W	75 %	8.22	n.d	0.17	n.d	0.25	n.d	13.8	16.6	15.2
	45 %	8.31		0.21		0.30				
	25 %	6.29		0.71		1.36				
	16 %	24.1		0.23		0.11				
	4 %	17.2		0.21		0.15				
	1 %	9.61		0.29		0.35				

* Integrated value measured at 75 % was excluded of the calculation.

BGD
11, 15053–15086, 2014

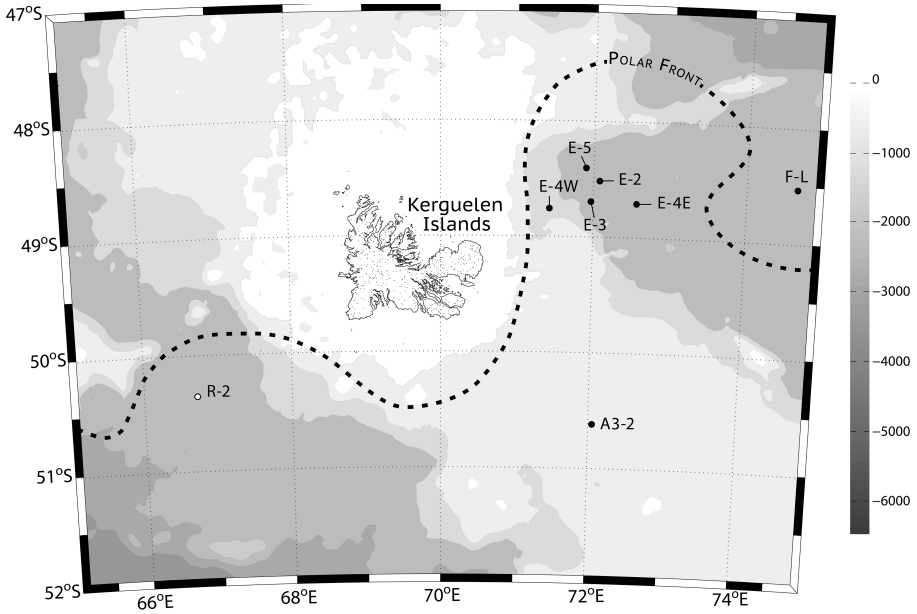

Figure 1. Map of KEOPS2 study area showing the stations sampled for Fe uptake experiments. Dashed line represents the position of the Polar Front. The base map shows the bathymetry in meters.

BGD
11, 15053–15086, 2014

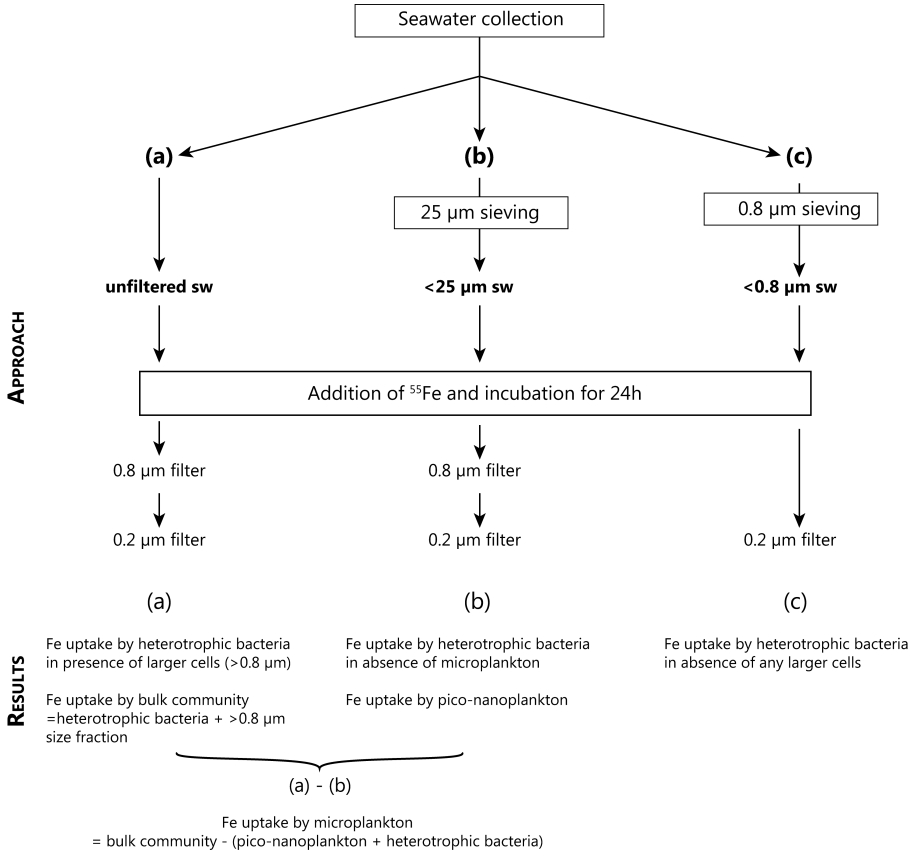

Figure 2. Schematic representation of experiments to determine Fe uptake by heterotrophic bacteria (0.2–0.8 µm), pico-nanoplankton (0.8–25 µm) and microplankton (> 25 µm) during the KEOPS2 cruise. Sw for seawater.

BGD
11, 15053–15086, 2014

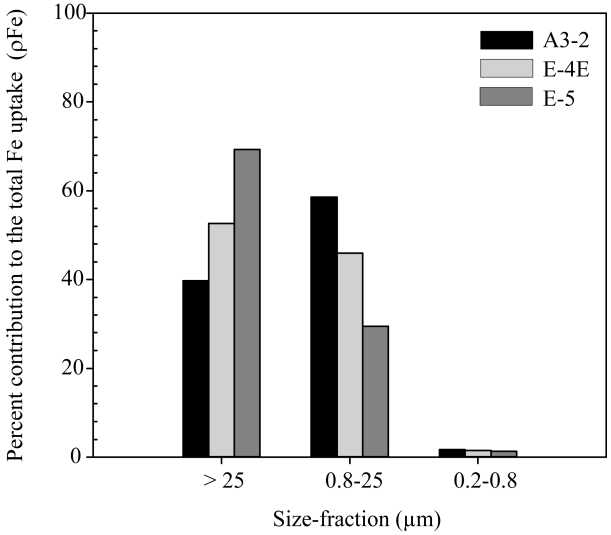

Figure 3. Relative contribution of different size-fractions to total Fe uptake. The percent contribution was calculated from Fe uptake fluxes integrated over the euphotic layer at plateau (A3-2) and downstream plume (E-4E and E-5) stations.

BGD
11, 15053–15086, 2014

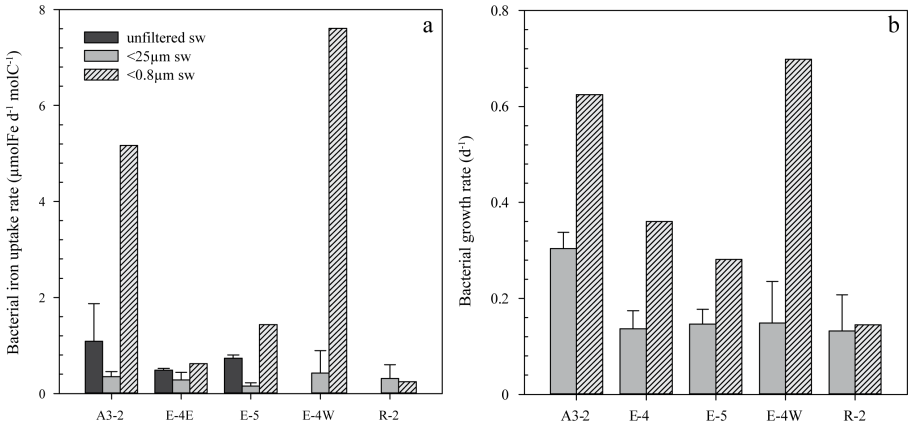

Figure 4. Bacterial Fe uptake normalized per carbon biomass **(a)** and bacterial growth rates **(b)** in incubations conducted with bulk community ($(\rho\mathrm{Fe}:\mathrm{POC})_{\mathrm{bact}}$, unfiltered seawater), in absence of microplankton ($(\rho\mathrm{Fe}:\mathrm{POC})_{\mathrm{bact}}^{<25\,\mu\mathrm{m}}$, < 25 µm seawater), and in the absence of these two size-fractions ($(\rho\mathrm{Fe}:\mathrm{POC})_{\mathrm{bact}}^{<0.8\,\mu\mathrm{m}}$, < 0.8 µm seawater). As no significant effect of light on Fe uptake was observed for any station we consider the values measured at the different levels of PAR as replicates. The bars for unfiltered seawater represents the average ± SD of the three light levels (75, 25 and 1 % of surface PAR). The bars for < 25 µm seawater represent the average ± SD of all the light levels (n = 6 for stations E-4E, E-5, and E-4W; n = 5 for stations A3-2 and R-2).

BGD
11, 15053–15086, 2014

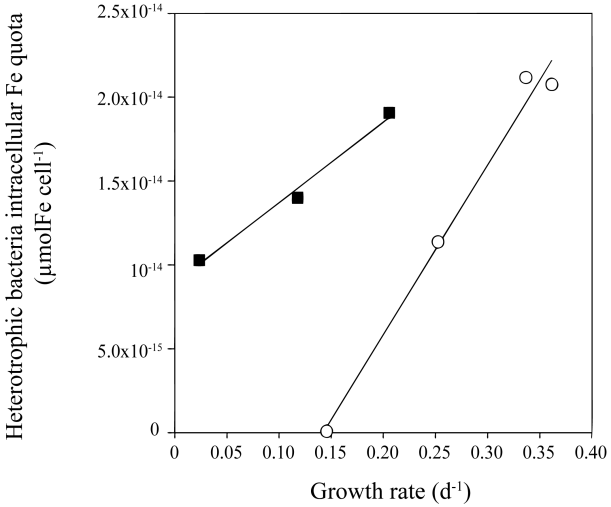

Figure 5. Relationship between the intracellular bacterial Fe quota and growth rate. Black squares: E-4W, E-5 and R-2 stations; regression line $r^2 = 0.99$, $y = 4.8 \times 10^{-14} + 8.9 \times 10^{-15}$. Grey circles: E-2, E-3, A3-2, and F-L stations; regression line $r^2 = 0.99$, $y = 10 \times 10^{-14} + 1.4 \times 10^{-15}$.

BGD
11, 15053–15086, 2014

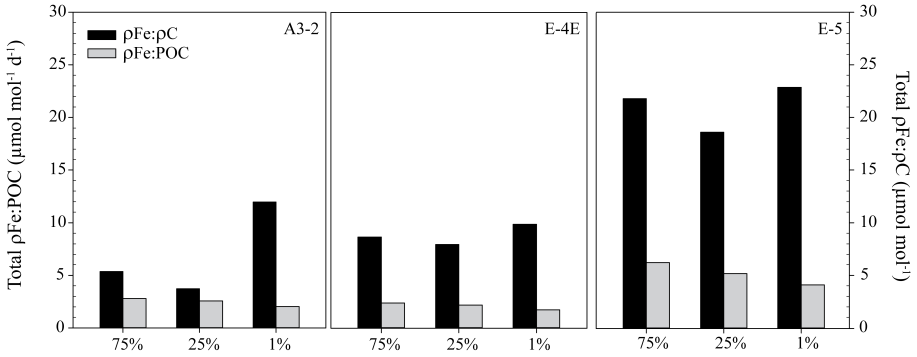

Figure 6. Comparison between total Fe : C uptake ratios noted ρFe : ρC (black bars) and Fe uptake by the bulk community normalized to carbon biomass noted ρFe : POC (grey bars) at 3 different surface PAR levels at stations A3-2 (plateau), E-4E and E-5 (plume).

BGD
11, 15053–15086, 2014

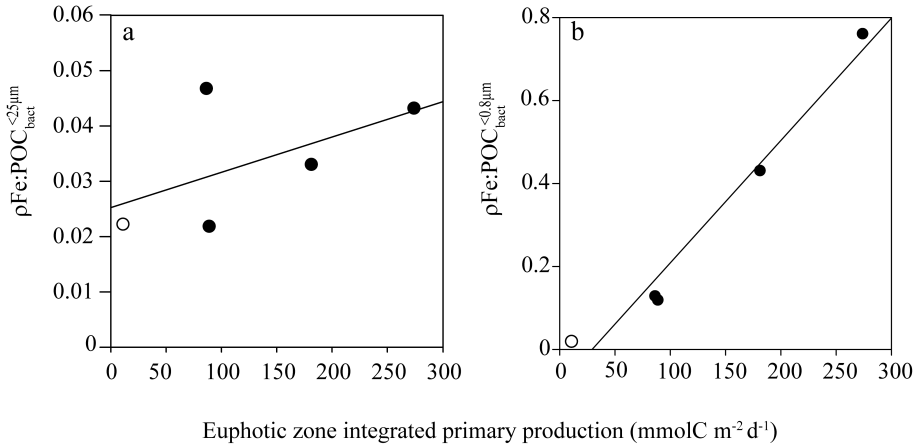

Figure 7. Relationship between the C-normalized bacterial Fe uptake in the absence of microplankton ($(\rho Fe:POC)^{<25\,\mu m}_{bact}$), **(a)** or in the absence of pico-nanoplankton ($(\rho Fe:POC)^{<0.8\,\mu m}_{bact}$), **(b)** and euphotic zone integrated primary production. The plotted line was obtained by least-square regression ($r^2 = 0.31$ with $p = 0.32$ and 0.97 with $p = 0.002$ for diagram **(a)** and **(b)**, respectively). Empty symbol represents the reference station R-2 and filled symbols are for Fe-fertilized stations.

BGD
11, 15053–15086, 2014